ARTICLE OPEN

Zero-energy pinning from interactions in Majorana nanowires

Fernando Domínguez[1], Jorge Cayao[3], Pablo San-Jose[3], Ramón Aguado[3], Alfredo Levy Yeyati[1] and Elsa Prada[2]

Majorana zero modes at the boundaries of topological superconductors are charge-neutral, an equal superposition of electrons and holes. This ideal situation is, however, hard to achieve in physical implementations, such as proximitized semiconducting nanowires of realistic length. In such systems Majorana overlaps are unavoidable and lead to their hybridization into *charged* Bogoliubov quasiparticles of finite energy, which, unlike true zero modes, are affected by electronic interactions. We here demonstrate that these interactions, particularly with bound charges in the dielectric surroundings, drastically change the non-interacting paradigm. Remarkably, interactions may completely suppress Majorana hybridization around parity crossings, where the total charge in the nanowire changes. This effect, dubbed zero-energy pinning, stabilizes Majoranas back to zero energy and charge, and leads to electronically incompressible parameter regions wherein Majoranas remain insensitive to local perturbations, despite their overlap.

INTRODUCTION

Since the early experimental efforts toward the generation and characterization of Majorana zero modes (MZMs) in nanowires,[1–5] remarkable progress has been accomplished.[6–8] Cleaner devices, with longer mean free paths and much more robust-induced superconductivity, are now available. Samples of this quality are expected to develop an unambiguous, topologically non-trivial superconducting phase hosting MZMs.[9] Owing to their non-Abelian statistics, braiding operations of MZMs are topologically protected and hold promise as the basis of fault-tolerant quantum computers.[10, 11]

Majoranas are topologically protected against local fluctuations in the environment inasmuch as they do not overlap spatially. However, deviations from this stringent condition always occur in realistic samples of finite length L, see Fig. 1a. In this case, the two MZMs at opposite ends of the wire overlap and become a charged Bogoliubov quasiparticle of finite energy ε_M and charge $Q_M < e$ (assuming a macroscopic and/or grounded parent superconductor; the case of a floating superconductor with charging energy has been studied in, e.g., refs [12, 13]). While these deviations are expected to be exponentially small, their importance of course depends on the spatial extension of the Majoranas ξ_M as compared to L (or the wire's mean free path, whichever is smaller), since both ε_M and Q_M decrease as $\sim e^{-L/\xi_M}$.

Even in the longer $L \sim 1\,\mu m$ nanowires experimentally studied so far, deviations from true MZM behavior are not negligible, since typically ξ_M is in the hundreds of nanometers. This theoretical expectation is in stark contrast with many experiments reporting surprisingly robust zero-bias anomalies (see, e.g., ref. [8]). Within a non-interacting picture,[14, 15] the only solution to this conflict is to assume values of the spin-orbit coupling much larger than the ones estimated for InAs or InSb NWs.[16] Apart from the exponential suppression, ε_M is expected to cross zero energy (parity crossings where Q_M changes) in an oscillatory fashion[17–19] as a function of

magnetic field, chemical potential, or length. Both the exponential suppression and the oscillatory behavior of ε_M have recently been demonstrated experimentally.[7] However, these experiments report on unexplained features in rather short wires with $L \sim \xi_M$ in the form of parity crossings that extend across a finite range of magnetic field (instead of point-like zero-energy crossings).

In this work, we present an alternative to the non-interacting view that provides an explanation to the above unresolved issues. By considering electronic interactions with the electrostatic environment,[20] we demonstrate that zero-energy crossings originating from the oscillatory splitting of overlapping MZMs are spontaneously stabilized into extended regions in parameter space wherein Majoranas become pinned to zero energy (Fig. 1c). Our results show that the absence of Majorana splittings, which is commonly identified with non-overlapping Majoranas with topological protection, can occur despite the Majorana overlap in nanowires of finite length.

The interactions involved in Majorana zero-energy pinning are not intrinsic to the wire,[18, 21–28] but rather extrinsic, between electrons that enter the wire and bound charges in the dielectric environment that arise in response. Our results suggest that such electronic interactions provide a powerful mechanism to stabilize Majorana-based qubits in realistic nanowires, and may account for the hitherto unexplained experimental features.[7, 8]

RESULTS

The central idea behind the zero-energy pinning phenomenon is the emergence of repulsive self-interactions through image charges in the dielectric medium. Before presenting full microscopic calculations, we first illustrate the mechanism with a toy example. Assume a quantum system with a single-particle state ψ_M that carries an electric charge Q_M. In the absence of interactions its energy is ε_M. The Hamiltonian, including a "self-interaction" term,

[1]Departamento de Física Teórica de la Materia Condensada, Condensed Matter Physics Center (IFIMAC) and Instituto Nicolás Cabrera, Universidad Autónoma de Madrid, Madrid E-28049, Spain; [2]Departamento de Física de la Materia Condensada, Condensed Matter Physics Center (IFIMAC) and Instituto Nicolás Cabrera, Universidad Autónoma de Madrid, Madrid E-28049, Spain and [3]Instituto de Ciencia de Materiales de Madrid, Consejo Superior de Investigaciones Científicas (ICMM-CSIC), Sor Juana Inés de la Cruz 3, Madrid 28049, Spain
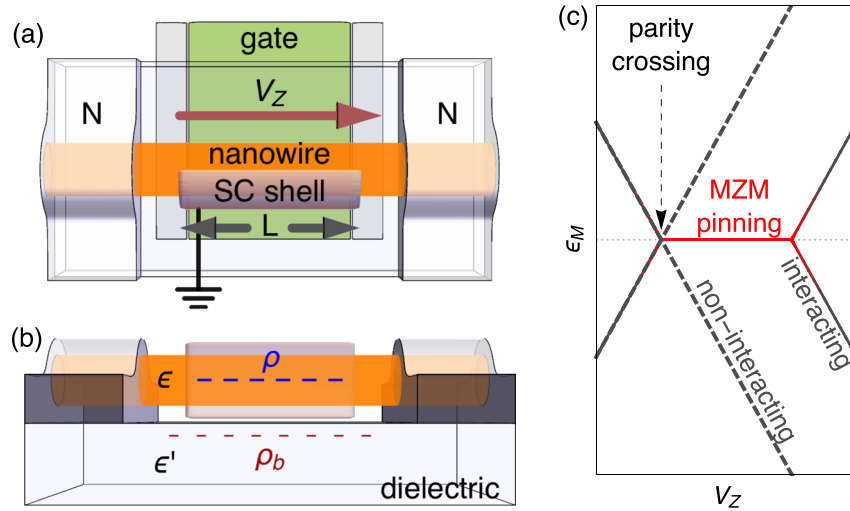Correspondence: Elsa Prada (elsa.prada@uam.es)

Fig. 1 **a** Proximitized Rashba nanowire of length L with gate-tunable Fermi energy μ and under a parallel Zeeman field V_Z. **b** Bound charges ρ_b arise in the dielectric surroundings, which interact with free charges ρ in the nanowire. **c** Sketch of the interaction-induced pinning, discussed in this work, of Majoranas at zero energy around parity crossings. This pinning provides a natural explanation to hitherto unresolved experimental features in Majorana wires (see, e. g., Fig. 3c in ref. 7)

takes the form $H = \varepsilon_M \psi_M^\dagger \psi_M + V_b Q_M \langle \psi_M^\dagger \psi_M \rangle \psi_M^\dagger \psi_M$, with eV_b an energy scale. Thus, in the presence of interactions, the effective level $\tilde{\varepsilon}_M$ is the self-consistent solution to $\tilde{\varepsilon}_M = \varepsilon_M + V_b Q_M f(\tilde{\varepsilon}_M)$, where $f(\varepsilon) = 1/(e^{\varepsilon/k_B T} + 1)$ is the Fermi function. As ε_M is externally tuned by a parameter V_Z to cross the Fermi energy (defined as zero), the resulting electron and hole energies $\pm \tilde{\varepsilon}_M$ with interactions (solid curves, $V_b > 0$ [repulsive]) and without (dashed, $V_b = 0$) are of the form shown in Fig. 1c for $T \to 0$. We see that the $V_b = 0$ parity crossing at $\varepsilon_M(V_Z) = 0$ transforms, for repulsive $V_b > 0$, into a finite plateau (in *red*), wherein $\tilde{\varepsilon}_M$ becomes pinned to zero within a finite range of V_Z, $0 < \varepsilon_M(V_Z) < V_b Q_M$. The pinning plateau is electronically incompressible, and is the result of thermal equilibrium combined with the self-interaction energy cost of occupying state ψ_M.

The above toy model for pinning presents a fundamental question when considering Majoranas in the role of the ψ_M state: how do physical self-interactions arise? It is clear that self-interactions of the form $\langle \psi_M^\dagger \psi_M \rangle \psi_M^\dagger \psi_M$ are unphysical in an isolated quantum system. In a generic basis, a direct (intrinsic) charge–charge interaction of the form $H_C = \sum_{ij} \psi_i^\dagger \psi_i V_{ij} \psi_j^\dagger \psi_j$ produces self-interaction of eigenstates when treated at the Hartree level, but this is canceled by the Fock correction.[29–31]

However, if the electronic system is immersed in a dielectric medium, a bound charge density $\rho_b(\mathbf{r})$ may appear, in response to electric charges $\hat{\rho}(r)$ in the system, at interfaces where the dielectric constant $\varepsilon(\mathbf{r})$ changes, see Fig. 1b. These $\rho_b(\mathbf{r})$ generate an electrostatic potential $\phi(\mathbf{r})$ that acts back onto $\hat{\rho}(\mathbf{r})$, such that the total potential $\phi_{tot}(\mathbf{r}) = \phi_{sys}(\mathbf{r}) + \phi(\mathbf{r})$ satisfies the inhomogeneous Poisson equation $\nabla \cdot [\varepsilon(r)\nabla\phi_{tot}(r)] = -4\pi\langle\hat{\rho}(r)\rangle$, and $\phi_{sys}(\mathbf{r})$ is the potential for an infinite system with a uniform ε (without bound charges). The resulting (extrinsic) interaction between the system's $\hat{\rho}(\mathbf{r})$ and bound charges $\rho_b(\mathbf{r}')$ then takes the form of a Hartee-like physical self-interaction, $\int \phi(r)\hat{\rho}(r) = \int V_b(r',r)\langle\hat{\rho}(r')\rangle\hat{\rho}(r)$, where V_b depends on the actual device geometry. Note that no Fock-like correction should be included here, since this is a purely classical effect: bound charges are located outside the nanowire and can be distinguished from the free charges. Thus, an effective Hamiltonian similar to the toy model above becomes relevant. Interaction with bound charges should be expected to produce zero-energy pinning of a quantum state as long as they are repulsive (i.e., if ρ_b and ρ have the same sign). The latter condition is satisfied if the dielectric environment has a smaller dielectric constant than the nanowire, the typical situation in most

experiments (e.g., InSb or InAs nanowires on a SiO$_2$ substrate, see the "Discussion" section for further details). Such self-interactions are well known in the context of molecular junctions,[32, 33] but, to our knowledge, their implications have not been explored in the context of Majorana wires.

A second relevant question concerns the charge Q_M associated to Majoranas. MZMs in infinite superconducting systems are charge-neutral, an equal superposition of electrons and holes. As such, it might come as a surprise that electronic interactions, which are sensitive to electronic charge, would have an effect on Majoranas. It was demonstrated,[34, 35] however, that the state resulting from the hybridization of two overlapping MZMs, each located at an end of a nanowire of length L, is not charge-neutral, but rather defines a charged Bogoliubov quasiparticle of finite energy ε_M and charge $Q_M < e$, with typical ε_M and Q_M decreasing exponentially as $\sim e^{-L/\xi_M}$. We now analyze this phenomenology in detail within a non-interacting model[14, 15] of a proximitized InSb semiconducting nanowire, oriented along the x-direction, of length $L = 1$ μm and subjected to a parallel Zeeman field $V_Z = g\mu_B B/2$ (g is the g-factor, μ_B is the Bohr magneton, and B is the magnetic field). The continuum Hamiltonian without superconductivity reads $H_0 = \hbar^2 k^2/2m + a\boldsymbol{\sigma}_y k + V_Z\boldsymbol{\sigma}_x$, where $\hbar k$ is the momentum along the wire, $\boldsymbol{\sigma}$ is the spin, the InSb spin-orbit coupling is $a = 0.2$ eV Å, and the effective mass is $m = 0.015\, m_e$. We include the induced superconducting pairing $\Delta = 0.5$ meV in the second-quantized Nambu representation,

$$H = \frac{1}{2}\int dx\, (\Psi^\dagger(x), \Psi(x)) \begin{pmatrix} H_0 - \mu & -i\boldsymbol{\sigma}_y\Delta^* \\ i\boldsymbol{\sigma}_y\Delta & \mu - H_0^* \end{pmatrix} \begin{pmatrix} \Psi(x) \\ \Psi^\dagger(x) \end{pmatrix},$$

where $\Psi(x) = (\Psi_\uparrow(x), \Psi_\downarrow(x))$ is the electron field, so that the charge density reads $\hat{\rho}(x) = e\sum_\sigma \Psi_\sigma^\dagger(x)\Psi_\sigma(x)$.

Figure 2a and b show the total charge in the nanowire $Q_{tot} = \int_0^L dx\langle\hat{\rho}(x)\rangle$ at zero temperature and the low-energy spectrum as a function of V_Z, respectively. Any given Bogoliubov quasiparticle eigenstate

$$\psi_n = \int_0^L dx[u_n(x)\Psi(x) + v_n(x)\Psi^\dagger(x)] \tag{1}$$

in the Nambu spectrum with energy $\varepsilon_n > 0$ contributes to $Q_{tot} = \Sigma_n Q_n$ with a charge

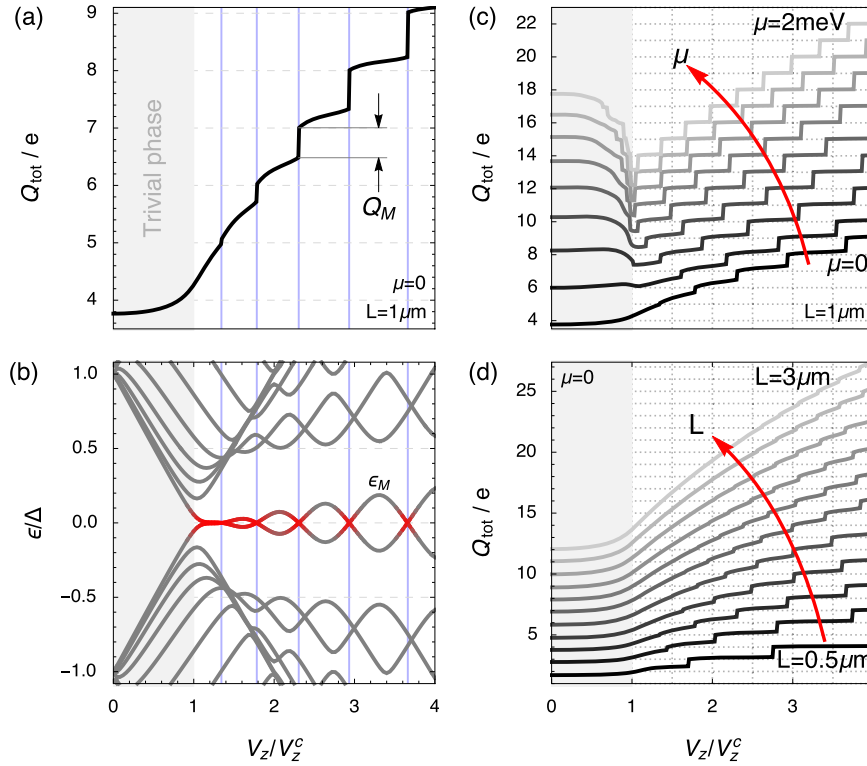$$Q_n = e\int_0^L dx\{f(\varepsilon_n)|u_n(x)|^2 + [1 - f(\varepsilon_n)]|v_n(x)|^2\}, \tag{2}$$

Fig. 2 **a** Total charge Q_{tot} in a non-interacting topological nanowire vs. V_Z. For $V_Z > V_Z^c$, Q_{tot} increases in jumps of magnitude $Q_M < e$ at parity crossings, shown in *red* in **b**. **c**, **d** Charge jumps become more (less) quantized as μ (L) increases

where $f(\varepsilon_n)$ is its occupation probability. For $V_Z > V_Z^c = \sqrt{\Delta^2 + \mu^2}$ the nanowire becomes topologically non-trivial and, for $L \rightarrow \infty$, develops MZMs at each end $\gamma_{L,R} = \gamma_{L,R}^\dagger$ with $u_{L,R}(x) = v_{L,R}^*(x)$. These states have zero charge, since changing their occupation does not change Q_{tot}. For finite L, the MZMs overlap and are no longer eigenstates, but hybridize into two special $n = \pm 1$ Nambu eigenstates $\psi_1 = \psi_M = (\gamma_L + i\gamma_R)/2$ and $\psi_{-1} = \psi_M^\dagger = (\gamma_L - i\gamma_R)/2$, whose energies $\pm \varepsilon_M$ oscillate around zero as a function of V_Z, μ, or L. Each time ε_M crosses zero in Fig. 2b (parity crossing), the zero-temperature occupation of the ψ_M quasiparticle at equilibrium changes abruptly, and the total charge of the wire experiences a non-quantized jump $Q_M = |Q_1 - Q_{-1}|$, as shown in Fig. 2a. Thus, the charge Q_M of the non-local Majorana fermion ψ_M is non-zero despite it being a superposition of the two neutral MZMs, and is distributed almost uniformly along the wire. It reads

$$
Q_M = \frac{e}{4} \int_0^L dx \left[|u_L^*(x) + iu_R^*(x)|^2 - |u_L^*(x) - iu_R^*(x)|^2 \right] =
$$
$$
e \int_0^L dx |u_L(x)u_R(x)|, \tag{3}
$$

i.e., Q_M is the spatial overlap of the two Majoranas (here we have chosen u_L real and u_R imaginary without loss of generality). As we have discussed in the "Introduction", the spatial extension of MZMs ξ_M is typically larger than the spin-orbit length $L_{\text{SO}} = \hbar^2/am$,[36] which is seldom smaller than a few hundred nanometers ($L_{\text{SO}} = 254$ nm here). In the weak SO regime, which corresponds to typical SO lengths for InSb nanowires of $L_{\text{SO}} \approx 250$ nm (SO coupling $a \sim 0.2$ eVÅ), the Majorana localization length is $\xi_M \sim L_{\text{SO}}$, and furthermore increases with Zeeman field.[37] The condition $L \gg \xi_M$ cannot be fulfilled as the Zeeman field exceeds the critical value above the topological transition. If, on the other hand, we assume stronger SO couplings, ξ_M saturates to $\xi_M \sim a/\Delta$,[16, 36] which, for typical values of Δ, is still much larger than the SO length. For example, assuming a SO coupling ten times larger than before, $a \sim 2$ eVÅ, and a proximity gap $\Delta = 0.5$ meV (of the order of the

experimental one in ref. 8), the Majorana localization length is $\xi_M \sim 400$ nm. The $L \gg \xi_M$ limit would therefore need much longer wires than the ones studied so far. Thus, even in rather long $L \sim 1$ μm non-interacting topological nanowires, the overlap of the Majoranas is sizeable, and results in large $Q_M \sim e$ charge jumps (see Fig. 2a).

Since parity-crossings introduce a charge Q_M into the system, they should be expected to give rise, in a repulsive dielectric environment, to bound charges of the same sign and hence to repulsive self-interactions and to zero-energy pinning of the corresponding MZMs. To demonstrate this effect we now add interactions to the above InSb Rashba nanowire model. Following the preceding discussion, we include only interactions with bound charges in the dielectric medium, described at a self-consistent Poisson mean field level. (The addition of intrinsic interactions do not change the essential results, and are analyzed in the Supplementary Information.) We replace H_0 in the non-interacting nanowire Hamiltonian H above with $H_0 + \phi(x)$, where the self-consistent potential created by bound charges is written as

$$
\phi(x) = \int dx' \, V_b(x, x') \langle \hat{\rho}(x') \rangle. \tag{4}
$$

We assume a simple geometry and a Coulomb interaction with image charges of the form

$$
V_b(x, x') \approx (\varepsilon - \varepsilon')/(\varepsilon + \varepsilon')/(4\pi\varepsilon_0\varepsilon((2R)^2 + |x - x'|^2)^{1/2}),
$$

where $\varepsilon = 17.7$ is the InSb dielectric constant, $\varepsilon' = 3.9$ is that of a SiO$_2$ substrate, and $R = 50$ nm is the nanowire radius (see Supplementary Information for a derivation). The results are qualitatively independent of the precise form of V_b, as long as it is repulsive ($\varepsilon > \varepsilon'$). We reabsorb the $V_Z = 0$ value of the potential $\phi(L/2)$ at the center of the nanowire into μ, so that the actual Fermi energy at zero magnetic field is equal to μ with and without interactions.

The potential $\phi(x)$ is solved numerically by self-consistent iteration (see the Supplementary Information for analytical results).
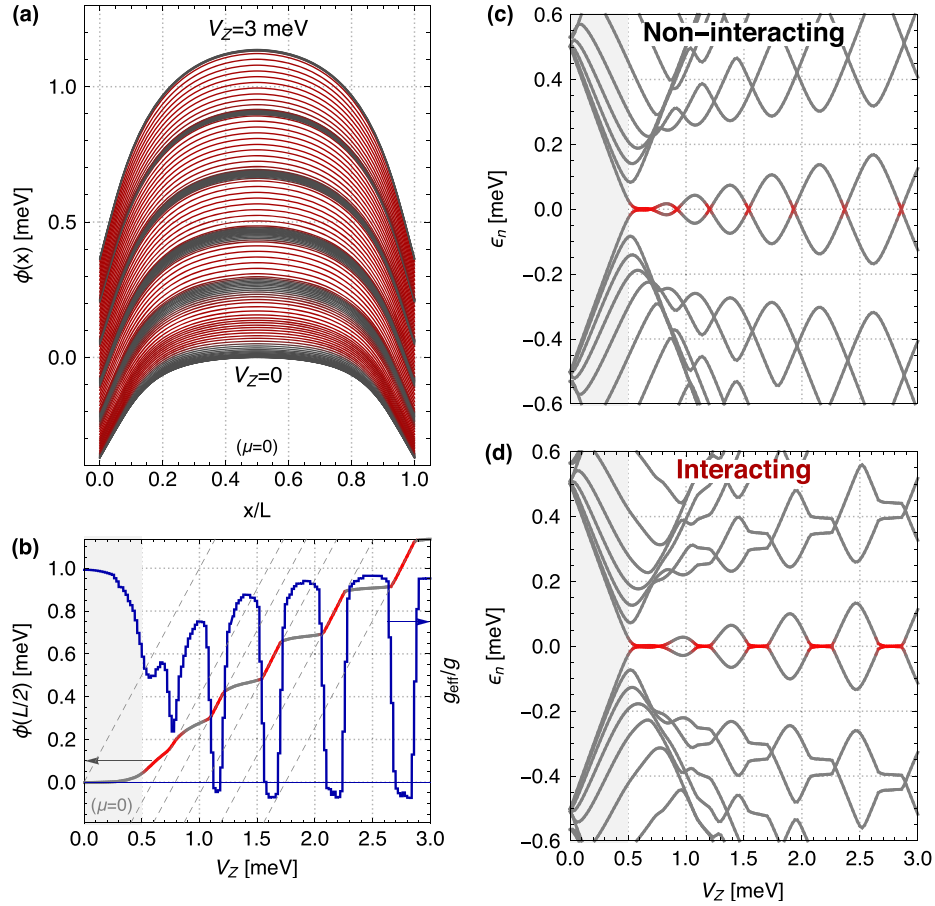
Fig. 3 **a** Screening potential $\phi(x)$ along a proximitized InSb nanowire of radius $R = 50$ nm and length $L = 1$ μm for increasing Zeeman field V_Z. We take $\Delta = 0.5$ meV and $\mu = 0$. Red (gray) curves correspond to an incompresible (compressible) regime. **b** Increase of the potential at the center of the wire $\phi(L/2)$ with V_Z, and the corresponding effective g-factor $g_{eff} = g[1 - \partial\phi(L/2)/\partial V_Z]$ (blue line). Intervals in red correspond to almost perfect screening of V_Z ($g_{eff} \approx 0$). **c, d** Non-interacting and interacting spectra of the nanowire. Note that perfect Zeeman screening by interactions is correlated with zero-energy pinnings of Majorana bound states (extended zero modes in red). An equivalent simulation to **d** including also intrinsic interactions in the nanowire is shown in Supplementary Material Fig. 1

The solution for $\mu = 0$ is shown in Fig. 3a as a function of V_Z, while $\phi(L/2)$ evaluated at the center of the nanowire is shown in Fig. 3b. The V_Z-dependent $\phi(L/2)$ transforms the simple non-interacting Fermi energy $\varepsilon_F = \mu + V_Z$ into a non-trivial $\varepsilon_F^{eff} = \mu + V_Z - \phi(L/2)$ at the center of the nanowire, changing also the V_Z-dependence of the spectrum as a result. Panels (c) and (d) show the corresponding low-energy spectrum without and with interactions, respectively. For $V_Z > V_Z^c = 0.5$ meV, parity crossings emerge in the non-interacting spectrum that inject a finite charge Q_M into the system (Fig. 2a). At each of these points, the interactions with bound charges conspire to suppress the charging, giving rise to finite intervals of V_Z with pinned zero-energy modes in place of parity crossings (panel (d)). These are the result of a rapid increase in the overall self-consistent $\phi(x)$ within each interval (red curves in panels (a, b)), which screens the Zeeman field in ε_F^{eff} almost completely, making the system incompressible $\partial\varepsilon_F^{eff}/\partial V_Z \approx 0$. This intermittent incompressibility is visible in Fig. 3b as a slope $\partial\phi(L/2)/\partial V_Z \approx 1$. The electronic compressibility against variations of V_Z may be quantified by the effective g-factor $g_{eff} = g \partial\varepsilon_F^{eff}/\partial V_Z = g[1 - \partial\phi(L/2)/\partial V_Z]$, in blue. Deviations from exact zero-energy pinning and perfect incompressibility $g_{eff} = 0$ may arise from finite temperature, $T = 10$ mK in these simulations, or finite decay rate into the reservoirs, neglected here.

In the above simulation the chemical potential was taken as $\mu = 0$. A similar phenomenology persist also at different electronic densities. Figure 4 shows the incompressible pinned regions (panels (a, b), in red) and total charge Q_{tot} in the nanowire (panels

(c, d)) across the full $\mu - V_Z$ parameter space, without and with interactions. When interactions are switched on, zero-measure parity crossings grow into extended areas of pinned MZMs, always separated by areas with finite MZM hybridization $|\bar{\varepsilon}_M| > 0$ (white). Along a given line within each incompressible area, the charge in the nanowire jumps by a finite, almost constant Q_M.

We note that, apart from stabilizing MZMs, interactions induce a change around $\mu = 0$ in the slope s of incompressible regions in the $\mu - V_Z$ plane, with $s = -1$ for $\mu < 0$ like in the non-interacting case, and $-1 < s < 0$ for $\mu > 0$. The incompressible regions are contours of constant ε_F^{eff},[36] so that $s = -g\kappa_{eff}/g_{eff}$ is a ratio between system's μ-compressibility $\kappa_{eff} = \partial\varepsilon_F^{eff}/\partial\mu$, and the V_Z-compressibility $g_{eff}/g = \partial\varepsilon_F^{eff}/\partial V_Z$ discussed above. While both are equal for $\mu < 0$, κ_{eff} becomes suppressed for $\mu > 0$, so that $s \approx -1/(1 + (v/\mu)^{1/2})$ for a constant $v \propto V_b^2$ related to the interaction strength (see Supplementary Information).

DISCUSSION

We have discussed a generic mechanism whereby electrostatic interactions with the dielectric surroundings stabilize zero-energy modes in a finite length Majorana nanowire. This zero-energy pinning effect is the result, within a self-consistent mean field, of a repulsive self-interaction of nanowire electrons that arises when its dielectric environment has a smaller dielectric constant than the nanowire itself. In a more general situation in which the charge screening by the normal contacts and the parent
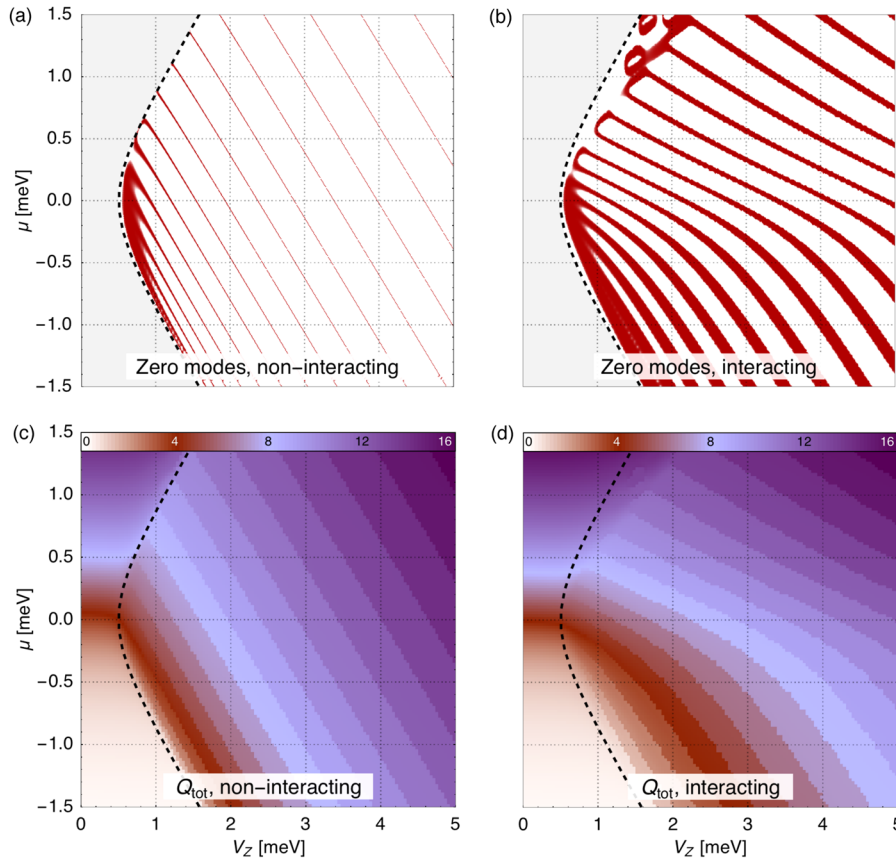
Fig. 4 Topological phase diagram of a non-interacting (**a**, **c**) and interacting (**b**, **d**), finite-length nanowire, see Fig. 3 for parameters. The *dashed line* corresponds to the non-interacting topological transition $V_Z^c = (\Delta^2 + \mu^2)^{1/2}$. *Red areas* in **a**, **b** represent zero-energy modes (with energy below 10 μeV at $T = 10$ mK), which correspond to narrow parity crossings from hybridized MZMs in **a**, and extended incompressible regions of MZMs pinned at zero energy in **b**. The total charge in the nanowire, panels **c**, **d**, increases by Q_M jumps at each zero-energy crossing

superconductor is also considered (a situation not presented here for simplicity, but with qualitatively similar results), the relevant quantity becomes the difference between the total electrostatic energy of a charge inside and outside the proximitized nanowire. This energy difference becomes positive, and hence self-interactions are repulsive, if charge screening is *reduced* upon entering the proximitized region. Such is the natural situation for nanowires with partial superconducting shells but full metallic covering at the contacts. The addition of charge into the nanowire calculated self-consistently then leads to pinning. Related dielectric-induced changes in addition energies have been discussed in molecular single electron transistors.[32] Zero-energy pinning cannot be captured by solving the electrostatic problem for infinite nanowires,[20] since it is necessary to take into account the electrostatic energy cost of adding charge at each parity crossing. Pinning, moreover, does not require a single channel regime. It also operates for any odd number of open channels,[38–40] as the physics of parity crossings is similar.

Within the stabilized regions in parameter space with pinned Majoranas, the system becomes electronically incompressible (a related phenomenon of global incompressibility, albeit unconnected to zero-energy pinning and parity crossings, was discussed in Majorana nanowires in the limit of strong intrinsic interactions[18]). As a result, potential fluctuations $\delta\mu$ from the environment or fluctuations δV_Z in the applied Zeeman field become screened out by interactions. This should remain true even for spatially non-uniform perturbations. As a result, the pinning effect could potentially be exploited to protect realistic Majorana-based qubits against environmental noise. We anticipate that, by

carefully engineering the dielectric surroundings of finite-length Majorana nanowires, one could exploit the electronic incompressibility of pinned regions to replace, at least partially, the topological protection of MZMs against decoherence, which is lost by their overlap. In this respect it is important to emphasize that pinned MZMs still overlap spatially, but become locked into degenerate parity eigenstates, regardless of any local perturbation, as long as thermal equilibrium is preserved. We should stress that, despite the common misconception in large part of the literature that identifies robust zero Majorana splitting with topological protection, it is non-locality what ultimately renders fermionic parity qubits immune to local noise. While there is a strong resemblance, the resilience to arbitrary perturbations discussed in this work is different from topological protection. The implications of pinning for the decoherence and relaxation times of parity-conserving Majorana qubits, such as, e.g., the $|00\rangle$ and $|11\rangle$ even-parity states of a four-Majorana setup, are non-trivial and should be the subject of future work.

The zero-energy pinning mechanism described in this work is generic, and is the result of the electrostatic energy cost from the interaction of the finite charge Q_M added to the nanowire at parity crossings and image charges in the dielectric environment. Given the generality of the mechanism, we speculate that the ideas discussed here are also relevant in other contexts, including parity crossings of Shiba states in non-topological superconductors.

METHODS

All the numerical results were computed within a self-consistent mean-field treatment of interactions in a tight-binding model for the

semiconducting nanowire. We used the MathQ framework[41] on a spatial discretization of the nanowire model $H_0 = \hbar^2 k^2 / 2m + a\boldsymbol{\sigma}_y k + V_Z \boldsymbol{\sigma}_x$. The lattice spacing used is 10 nm. The mean field self-consistency condition, encoded in Eq. (4), is achieved by iteration with an adaptive update coefficient. This is required at low temperatures to achieve convergence around pinned regions.

AUTHOR CONTRIBUTIONS

F.D., J.C., P.S-J., and E.P. performed the calculations. P.S-J. developed the *MathQ* computational framework. All authors contributed to the discussion, the design of the research, the analysis of the results, and the writing of the manuscript.

COMPETING INTERESTS

The authors declare no competing interest.

REFERENCES

1. Mourik, V. et al. Signatures of Majorana fermions in hybrid superconductor-semiconductor nanowire devices. *Science* **336**, 1003–1007 (2012).
2. Deng, M. T. et al. Anomalous zero-bias conductance peak in a Nb–InSb nanowire–Nb hybrid device. *Nano. Lett.* **12**, 6414–6419 (2012).
3. Das, A. et al. Zero-bias peaks and splitting in an al-inas nanowire topological superconductor as a signature of Majorana fermions. *Nat. Phys.* **8**, 887–895 (2012).
4. Churchill, H. O. H. et al. Superconductor-nanowire devices from tunneling to the multichannel regime: zero-bias oscillations and magnetoconductance crossover. *Phys. Rev. B* **87**, 241401 (2013).
5. Lee, E. J. H. et al. Spin-resolved andreev levels and parity crossings in hybrid superconductor-semiconductor nanostructures. *Nat. Nano.* **9**, 79–84 (2014).
6. Chang, W. et al. Hard gap in epitaxial semiconductor–superconductor nanowires. *Nat. Nano.* **10**, 232–236 (2015).
7. Albrecht, S. M. et al. Exponential protection of zero modes in Majorana islands. *Nature* **531**, 206–209 (2016).
8. Zhang, H. et al. Ballistic Majorana nanowire devices. *arXiv:1603.04069v1* (2016).
9. Kitaev, A. Y. Unpaired Majorana fermions in quantum wires. *Phys. Usp* **44**, 131 (2001).
10. Nayak, C., Simon, S., Stern, A., Freedman, M. & Das Sarma, S. Non-Abelian anyons and topological quantum computation. *Rev. Mod. Phys.* **80**, 1083–1159 (2008).
11. Sarma, S. D., Freedman, M. & Nayak, C. Majorana zero modes and topological quantum computation. *NPJ Quantum Inf.* **1**, 15001 EP (2015).
12. Fu, L. Electron teleportation via Majorana bound states in a mesoscopic superconductor. *Phys. Rev. Lett.* **104**, 056402 (2010).
13. Hützen, R., Zazunov, A., Braunecker, B., Yeyati, A. L. & Egger, R. Majorana single-charge transistor. *Phys. Rev. Lett.* **109**, 166403 (2012).
14. Lutchyn, R. M., Sau, J. D. & Das Sarma, S. Majorana fermions and a topological phase transition in semiconductor-superconductor heterostructures. *Phys. Rev. Lett.* **105**, 077001 (2010).
15. Oreg, Y., Refael, G. & von Oppen, F. Helical liquids and Majorana bound states in quantum wires. *Phys. Rev. Lett.* **105**, 177002 (2010).
16. Mishmash, R. V., Aasen, D., Higginbotham, A. P. & Alicea, J. Approaching a topological phase transition in Majorana nanowires. *Phys. Rev. B* **93**, 245404 (2016).
17. Prada, E., San-Jose, P. & Aguado, R. Transport spectroscopy of *ns* nanowire junctions with Majorana fermions. *Phys. Rev. B* **86**, 180503(R) (2012).
18. Das Sarma, S., Sau, J. D. & Stanescu, T. D. Splitting of the zero-bias conductance peak as smoking gun evidence for the existence of the Majorana mode in a superconductor-semiconductor nanowire. *Phys. Rev. B* **86**, 220506 (2012).
19. Rainis, D., Trifunovic, L., Klinovaja, J. & Loss, D. Towards a realistic transport modeling in a superconducting nanowire with Majorana fermions. *Phys. Rev. B* **87**, 024515 (2013).
20. Vuik, A., Eeltink, D., Akhmerov, A. R. & Wimmer, M. Effects of the electrostatic environment on the Majorana nanowire devices. *New J. Phys.* **18**, 033013 (2016).
21. Stoudenmire, E. M., Alicea, J., Starykh, O. A. & Fisher, M. P. Interaction effects in topological superconducting wires supporting Majorana fermions. *Phys. Rev. B* **84**, 014503 (2011).
22. Lutchyn, R. M. & Fisher, M. P. A. Interacting topological phases in multiband nanowires. *Phys. Rev. B* **84**, 214528 (2011).
23. Sela, E., Altland, A. & Rosch, A. Majorana fermions in strongly interacting helical liquids. *Phys. Rev. B* **84**, 085114 (2011).
24. Gangadharaiah, S., Braunecker, B., Simon, P. & Loss, D. Majorana edge states in interacting one-dimensional systems. *Phys. Rev. Lett.* **107**, 036801 (2011).
25. Fidkowski, L., Alicea, J., Lindner, N. H., Lutchyn, R. M. & Fisher, M. P. A. Universal transport signatures of Majorana fermions in superconductor-luttinger liquid junctions. *Phys. Rev. B* **85**, 245121 (2012).
26. Manolescu, A., Marinescu, D. C. & Stanescu, T. D. Coulomb interaction effects on the Majorana states in quantum wires. *J. Phys.: Condens. Matter* **26**, 172203 (2014).
27. Ghazaryan, A. & Chakraborty, T. Long-range coulomb interaction and Majorana fermions. *Phys. Rev. B* **92**, 115138 (2015).
28. Xu, H., Xiong, Y. & Wang, J. Topological phases and transport properties of screened interacting quantum wires. *Phys. Lett. A* **380**, 3534–3540 (2016).
29. Cowan, R. D. Atomic self-consistent-field calculations using statistical approximations for exchange and correlation. *Phys. Rev.* **163**, 54–61 (1967).
30. Perdew, J. P. & Zunger, A. Self-interaction correction to density-functional approximations for many-electron systems. *Phys. Rev. B* **23**, 5048–5079 (1981).
31. Anisimov, V. I. *Strong Coulomb Correlations in Electronic Structure Calculations* (CRC Press, 2000).
32. Kaasbjerg, K. & Flensberg, K. Strong polarization-induced reduction of addition energies in single-molecule nanojunctions. *Nano. Lett.* **8**, 3809–3814 (2008).
33. Kaasbjerg, K. & Flensberg, K. Image charge effects in single-molecule junctions: breaking of symmetries and negative-differential resistance in a benzene single-electron transistor. *Phys. Rev. B* **84**, 115457 (2011).
34. Ben-Shach, G. et al. Detecting Majorana modes in one-dimensional wires by charge sensing. *Phys. Rev. B* **91**, 045403 (2015).
35. Lin, C. H., Sau, J. D. & Das Sarma, S. Zero-bias conductance peak in Majorana wires made of semiconductor/superconductor hybrid structures. *Phys. Rev. B* **86**, 224511 (2012).
36. Klinovaja, J. & Loss, D. Composite Majorana fermion wave functions in nanowires. *Phys. Rev. B* **86**, 085408 (2012).
37. Cayao, J., Prada, E., San-Jose, P. & Aguado, R. SNS junctions in nanowires with spin-orbit coupling: role of confinement and helicity on the subgap spectrum. *Phys. Rev. B* **91**, 024514 (2015).
38. Potter, A. C. & Lee, P. A. Engineering a *p+ip* superconductor: comparison of topological insulator and rashba spin-orbit-coupled materials. *Phys. Rev. B* **83**, 184520 (2011).
39. Stanescu, T. D., Lutchyn, R. M. & Das Sarma, S. Majorana fermions in semi-conductor nanowires. *Phys. Rev. B* **84**, 144522 (2011).
40. San-Jose, P., Prada, E. & Aguado, R. Mapping the topological phase diagram of multiband semiconductors with supercurrents. *Phys. Rev. Lett.* **112**, 137001 (2014).
41. San-Jose, P. MathQ, a Mathematica package for the simulation of quantum systems, www.icmm.csic.es/sanjose/MathQ/MathQ.html.